

Carbon black · Reinforcement · Surface structure · Atomic force microscope (AFM) · Lateral force microscope (LFM)

Ruß · Verstärkerwirkung · Oberflächenstruktur · Kraftmikroskop (AFM) · Reibungsmikroskop (LFM)

Using the optical lever technique we have developed an atomic force microscope (AFM) which can also detect the friction force. In contrast to the scanning tunneling microscope (STM) the AFM is able to measure both conductive and nonconductive surfaces at resolutions down to the atomic level.

This technique has been applied to two carbon blacks (N110, N762) produced by oilfurnace process. The structural investigations of carbon black particles with the AFM show quasi-spheroidal particles fused together to form aggregates. The measured diameters of the particles are in good agreement with the data of the manufacturer. At higher magnification of the particle surface the images show individual particles consisting of graphite layer stacks organized in a concentric way around the center of the particle. A step-like structure of the surface is clearly shown by the AFM, arising from layer stacks tilted with respect to each other. The lateral size of the layers changes with the variation of the investigated carbon blacks. A value of 1.0–1.5 nm was found for the lateral layer size of N110 and 1.8–2.5 nm for N762. The lateral dimensions and the tilt of the graphite layer stacks could be significant parameters with regard to the reinforcing effect of carbon black.

Die Mikrostruktur von Ruß untersucht mit dem Kraftmikroskop

Basierend auf dem Lichtzeigerprinzip entwickelten wir ein Kraftmikroskop (AFM), das auch Reibungskräfte detektieren kann. Im Gegensatz zum Rastertunnelmikroskop (STM) kann das AFM sowohl leitende als auch nicht leitende Oberflächen mit atomarer Auflösung untersuchen.

Diese Technik wurde auf zwei Rußsorten (N110, N762) angewandt, die durch einen Ölfurnaceprozeß hergestellt worden sind. Die Strukturuntersuchungen der Rußpartikel mit dem AFM zeigen nahezu kugelförmige Partikel, die zu Aggregaten zusammengebacken sind. Die ermittelten Teilchendurchmesser stimmen mit den Herstellerangaben sehr gut überein. Eine Vergrößerung der Partikeloberfläche zeigt, daß jedes einzelne Partikel aus Graphitstapeln aufgebaut ist, die konzen-

W. Niedermeier, H. Raab, J. Stierstorfer, S. Kreitmeier and D. Göritz, Regensburg (FRG)

The Microstructure of Carbon Black Investigated by Atomic Force Microscopy

trisch um das Partikelzentrum angeordnet sind. Mit dem AFM konnte deutlich eine stufenartige Struktur aufgelöst werden, die von gegeneinander verkippten Graphitstapeln herrührt. Die laterale Ausdehnung der Plättchen variiert mit der Rußsorte und beträgt 1.0–1.5 nm für N110 bzw. 1.8–2.5 nm für N762. Die Ausdehnung und die Verkipfung der Graphitstapel könnten signifikante Parameter für den Verstärkungsmechanismus von Ruß sein.

1 Introduction

Elastomers as modern materials can be obtained with tailor-made properties by selection of rubber matrix, crosslinking agent and active fillers. The matrix may be a homopolymer or a blend of several polymers. The properties of the end product are determined by the original properties of the components and their mutual coupling behavior. The significance of boundary forces has indeed been recognized, but the mechanism of the interaction between the individual phases remains largely unknown [1, 2]. In particular, the question of the type of interaction between the rubber chains and the carbon black surface has yet to be explained.

To understand the reinforcing effect, the microstructure of the carbon black surface seems to be important. Carbon black fillers interact with their surroundings by means of their surfaces which are very large due to the small size of the carbon black particle [3]. Structural investigations in the nanometer region are necessary in order to get supplement information on the surface structure of carbon black obtained by conventional methods. If carbon black particles are embedded in a rubber matrix, the surface structure can be analysed using an atomic force microscope (AFM) [4]. The idea of a scanning probe technique for imaging both conductive and nonconductive surfaces led to the creation of the

AFM [5], five years after the appearance of the scanning tunneling microscope (STM) [6]. The principle of the AFM is to bring a sharp tip, located at the end of a microfabricated cantilever, into close proximity with the sample, and to move this fine tip over the sample to map the contours of the surface. The interatomic force between tip and surface is detected by measuring the deflection of a flexible cantilever. The AFM can profile surfaces similar to the STM at resolutions down to the atomic level.

2 Experimental

2.1 AFM design

The instrument we worked with is a variation of an earlier STM [7] which can be used as an AFM or a STM now. The design of our atomic force microscope is sketched in *Figure 1*. The centre of our instrument is formed by a stainless steel block (14.5 × 6 × 5 cm) with a slit of 1 cm. Two invar manufactured differential screws are used for the mechanical approach. The sample is mounted on a single tube piezo scanner fixed to the differential screw 1. Differential screw 1 provides the rough approach (50 µm per turn) towards the tip. The fine approach is obtained by the second differential screw (DS 2), positioned at the end of the steel block. So the small lift is reduced again by the decreasing spread along the slit and the gap can be mechanically controlled within very high accuracy (better than 5 nm). This accuracy is sufficient to bring the sample close enough to the cantilever to allow the piezoelectric transducer [8] to accomplish the final approach.

To detect the vertical motion of the tip which is proportional to the force applied to the surface of the sample by the tip, we use an optical deflection system. A light beam of a laser diode is focused on the backside of the lever. A four segment photodiode detects the deflection of the

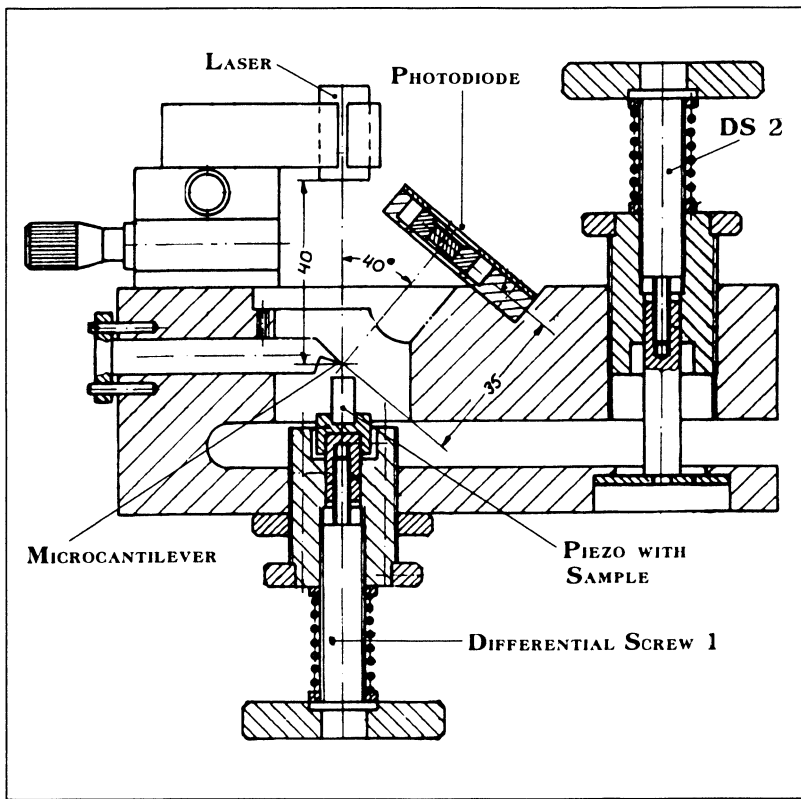


Figure 1. Schematic view of the AFM

cantilever by sensing the position of the reflected beam. With this setup, cantilever displacements of less than 0.1 nm are measurable [10]. Due to the geometric arrangement, the limiting factor of the vertical resolution is not the sensitivity of the photodiode but rather the sound and building vibrations. The effective noise level is approximately 0.04 nm root-mean-square in the frequency range from 10 Hz to 1 kHz.

2.2 Methods and material

Many new types of scanning heads basing upon the AFM principle exist now. In its simplest form, the AFM acts as a "miniature surface profilometer" and provides topographical images. One of the most interesting operation modes is the lateral force or friction mode, developed by *Mate et al.* [11] and *Erlandsson et al.* [12]. It is based on the frictional resistance of the probe while scanning the sample. *O. Marti et al.* [13] modified an AFM to measure simultaneously the force normal to the sample surface and the friction force arising from scanning. The lateral force induces a mechanical moment on the cantilever, which causes a deflection of the light beam in the x-direction, in addition to the deflection in the y-direction by the normal or repulsive force. By using a four quadrant photodiode the deflection due to the friction force and the deflection due to the normal force can be recorded simultaneously and independent of each other (Figure 2).

The sensitivity of this instrument was demonstrated on the surface of mica.

Both imaging modes have the potential for atomic resolution [13]. *O. Marti et al.* showed that the lateral force microscope (LFM) is sensitive to the chemical of the surface and may probably open new frontiers in tribology. Preliminary experiments in their laboratory confirm that soft samples might be imaged with better resolution in friction mode than in topography.

Therefore we modified our AFM in a similar manner (Figure 2) to measure simultaneously the topography and friction force and to correlate the friction image

with the topographical features of the sample surface. With this setup we can get new and better information than by a conventional AFM image based on topography. This new imaging mode will produce major advances in the analysis of carbon black and especially of carbon black-polymer composites.

In order to achieve high resolution the AFM is usually operated in the repulsive mode [14], which is also the mode used to determine friction coefficients. All reported measurements have been performed with repulsive forces in the range of $5 \cdot 10^{-9} - 1 \cdot 10^{-8}$ N. The topography of the surface was mapped in the constant-force mode. For the simultaneous measurement of the normal force and friction force we used rectangular Si cantilevers with a lever force constant of 0.11 N/m, a tip with a radius of curvature less than 10 nm and a length of 238 μm [15]. All other experiments were carried out with triangular Si_3N_4 cantilevers with a lever force constant of 0.06 N/m, a tip with a radius of curvature less than 40 nm and a length of 200 μm [16].

The samples were prepared by dispersing carbon black in hot toluene ultrasonically in order to scatter the carbon black agglomerates into aggregates and to eliminate the adsorbed polyaromatic compounds. Afterwards a droplet (about 0.03 ml) of this dispersion was placed upon a freshly cleaved mica surface and dried for 2 days. We used mica as substrate because of its atomic flat surface. In this way we avoided superposition of two topographical surfaces.

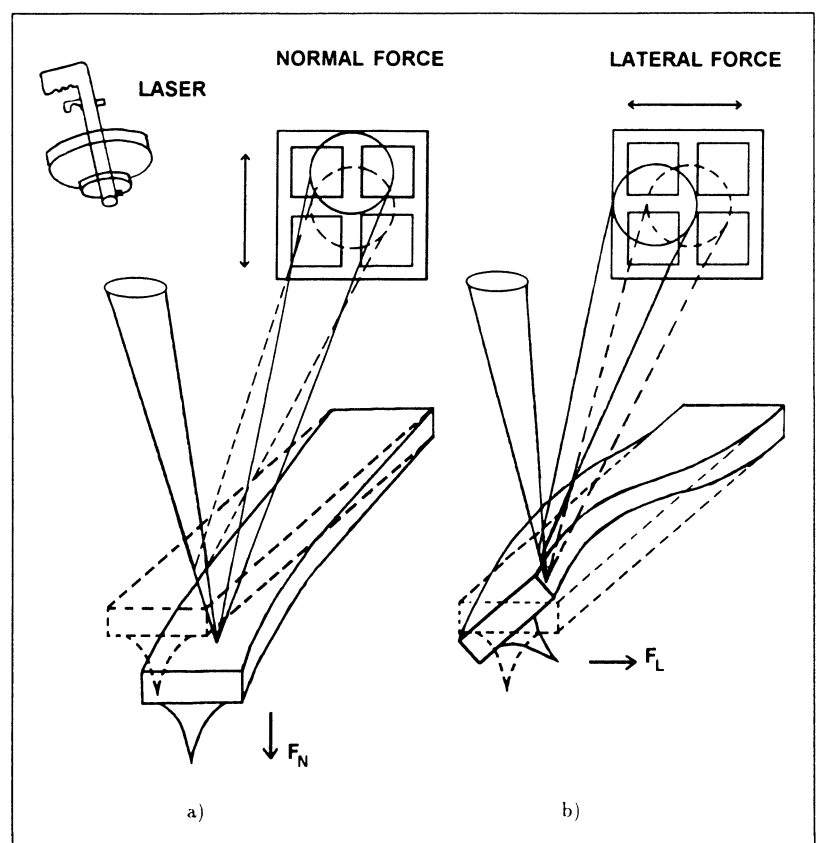


Figure 2. Schematic drawing for the simultaneous measurement of normal and lateral forces: a) An attractive force bends the lever upwards, deflecting the reflected light beam in the y-direction. b) A lateral force twists the lever, deflecting the reflected light beam in the x-direction.

Table 1. Characteristic description of carbon black: Arithmetic average of the particle diameter, surface area by nitrogen and crystallographic dimensions of the graphite layer stacks [18, 19]

Type of carbon black	Average diameter	Nitrogen surface area [$\frac{m^2}{g}$]	Crystallographic dimensions	
	[nm]		L_a [nm]	L_c [nm]
N110	18	130	2.01	1.44
N330	30	80	2.11	1.49
N550	45	40	2.23	1.65
N762	70	30	2.36	1.74

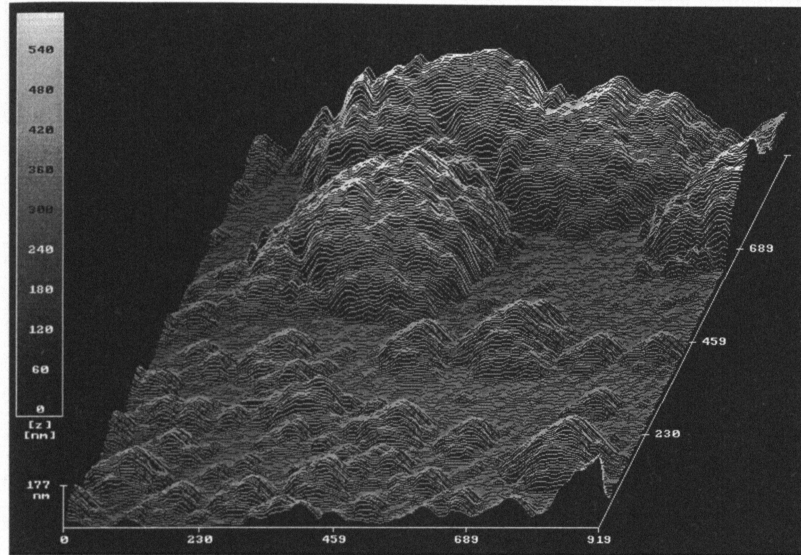


Figure 3. AFM image of a typical surface topography of N762 carbon black on mica. The composition of carbon black agglomerates of primary particles and separated particles can be seen. The particle diameter is 65–75 nm. The grey scale chart covers 540 nm; scan area is $919 \times 919 \text{ nm}^2$.

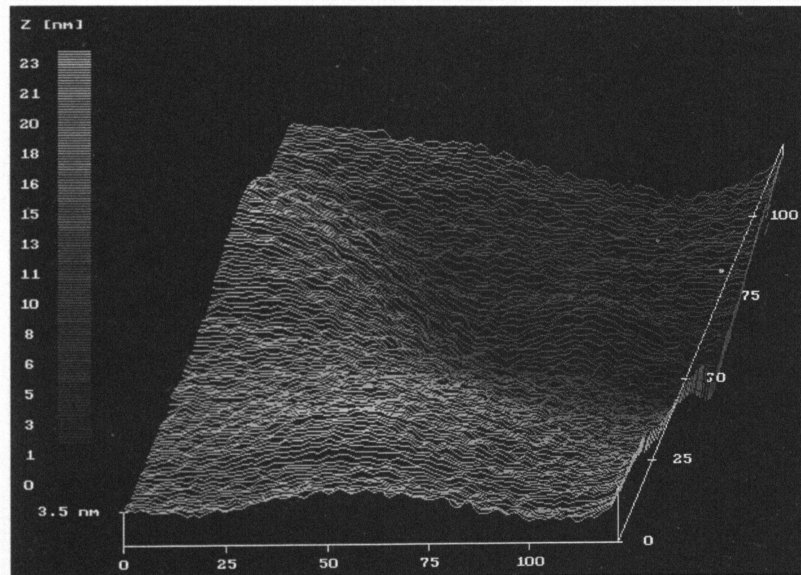


Figure 4. $(123 \text{ nm})^2$ – scan of two N762 carbon black. The grey scale spectrum covers 23 nm; reference height is 3.5 nm (left bottom corner).

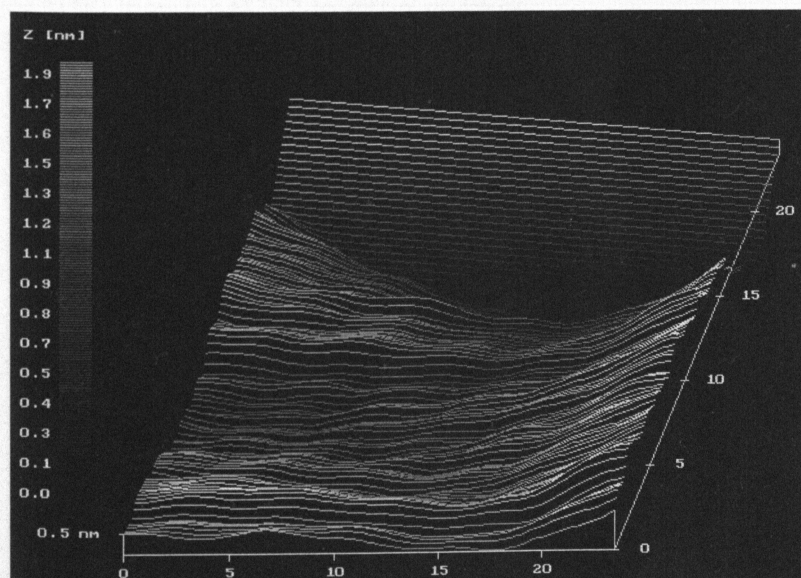


Figure 5. $(24 \text{ nm})^2$ – scan of the surface of a N762 particle with tilted domains of about 2 nm extension in the lateral direction. The grey scale spectrum covers 1.9 nm; reference height is 0.5 nm.

3 Results and discussion

Table 1 gives an overview of the investigated carbon blacks, manufactured by furnace technique [17]. The first column specifies the average diameter of the primary particles; the second column gives the surface area by nitrogen and the third and fourth show the crystallographic dimensions L_c and L_a obtained by X-ray refraction analysis [18, 19]. Reference values for N330 and N550 are also shown to demonstrate the increase of crystallographic dimensions with particle size. Generally, the value of the specific surface is higher for more reinforcing carbon blacks. The smaller the average diameter of primary particles, the better the reinforcing mechanism. The structure of the aggregates (clustered, branched or filamentous) is a geometric factor which influences also the rubber reinforcement.

3.1 Surface structure of N762

Carbon black morphology can be determined by particle size and shape. Furnace and thermally produced carbon blacks have been reported to be composed of nearly spheroidal particles. Figure 3 shows a typical large-scale image of N762. The height scale is represented by a grey scale chart. Thus, the complete information concerning the correlation, lateral and height extensions of the surface topography can be easily obtained from the same picture. The structure of carbon black consisting of quasi-spherical single particles and agglomerates composed of interpenetrating particles is clearly shown. The particle diameter varies between 65–75 nm which is consistent with the data of the manufacturer and previous observations by TEM [9].

To get more information about the surface structure of N762 we made small scans on two individual particles. The result of scanning a small area, $123 \times 123 \text{ nm}^2$, is displayed in Figure 4. The top of every particle can be recognized by the white spots.

The small visible surface roughness is no vibration or superposition of the electronic feedback [10]. The observed surface topography suggests tilted domains of graphite structures.

At a higher level of magnification (Figure 5) the surface forms a step-like structure. This arrangement, which covers all the carbon black surface, arises from tilted graphite layer stacks. To study the microstructure in more detail, eleven scan lines of the AFM image in Figure 5 are shown graphically in Figure 6. Since the spacing between two scan lines is

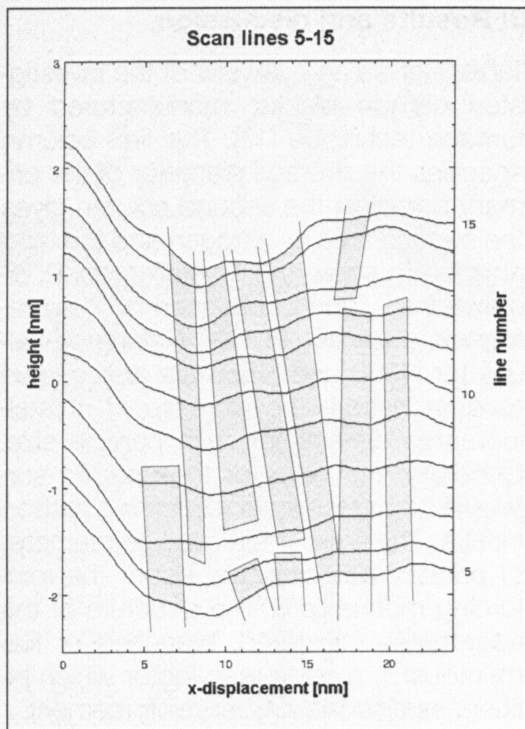


Figure 6. Eleven scan lines from AFM image of N762 particle surface in Figure 5. The spacing between the scan lines is about 0.2 nm. The dashed lines illustrate the crystallite planes in top plan view to visualize the real surface.

approximately 0.2 nm, the distance between the first and the last scan line is only 2.2 nm; the x-range is 24 nm. This different scaling is the reason for the elongated shape of the graphite planes shown in Figure 6. It can be used to imagine the lateral arrangement of the crystallites on the real surface. The dashed lines hint the contours of the crystallite planes. The similarity of single sections of adjacent scan lines determines the arrangement of the planes. If this parallel structure disappears from one to another scan line, a change of crystallites takes place. The sketch gives an idea of the tilt

Figure 8. Amplitude of the 10th scan line from AFM image at N762 particle surface shown in Figure 9. The dashed lines illustrate the crystallites in vertical view. The vertical extensions of the steps are about 0.1–0.3 nm, the lateral extensions are about 2 nm.

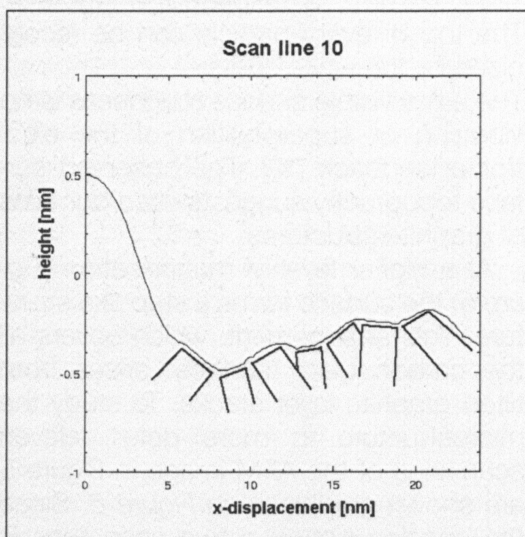
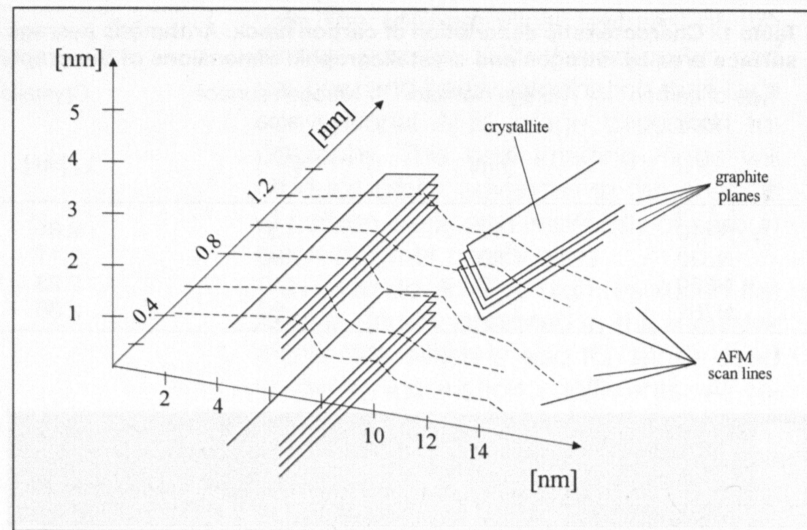


Figure 7. The dashed lines symbolize schematic scan lines of an AFM on tilted crystallites. A change in the parallelism of the scan lines indicates the beginning of another crystallite.



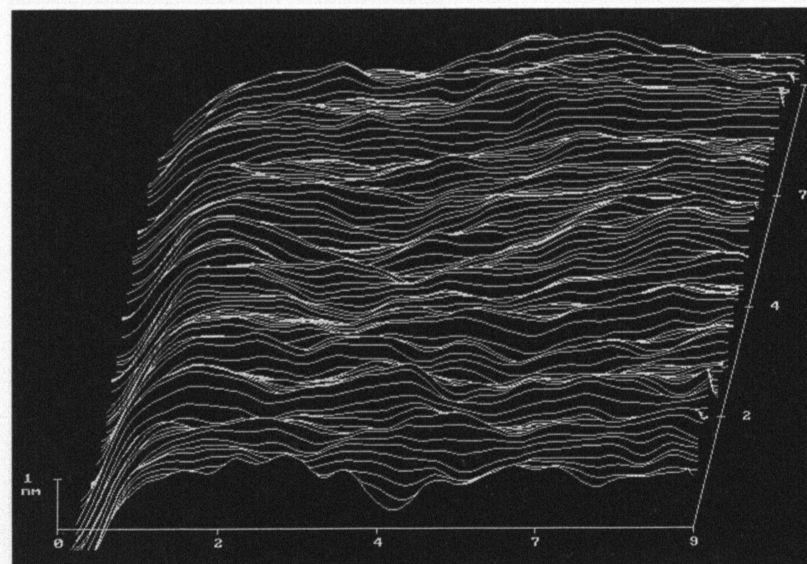
of the crystallites. The lateral extensions could be estimated to about 1.8–2.5 nm. This is in good accordance with the crystallographic dimension L_a of 2.36 nm (Table 1).

Figure 7 shows schematically the scan lines of an AFM made on tilted crystallites of graphite planes. This picture is designed to give a clearer imagination of the measured surface and to illustrate our interpretation of Figure 6.

Figure 8 displays the 10th scan line of Figure 5 to point out the tilt of the crystallites and to give an estimation of the vertical dimensions of the tilt. The vertical dimensions are usually in the order of 0.2–0.4 nm, corresponding to the thickness of a graphite plane, but partial the vertical dimensions range up to 1.5–2 nm, corresponding to the extension of a crystallite.

The microstructure of N762 is clearly shown in a more enlarged image in Figure 9 of a portion of the region in Figure 4. The surface roughness of the particles, arising from the crystallites, can be recognized. The rounded edges of the crystallites result from the radius of curvature of the tip.

Figure 9. High resolution image of a portion of the region shown in Figure 4. The microstructure of the surface arises from tilted graphite layer stacks with respect to each other. The lateral extensions can be estimated to be about 1.8–2.5 nm; vertical extensions are about 0.2–0.4 nm; scan area is $9 \times 9 \text{ nm}^2$; reference height is 1 nm.



3.2 Surface structure of N110

The single particle diameter of carbon black N110 is only 15–20 nm, therefore the surface activity is high favoring the agglomeration of particles. In spite of the small diameter of the single particles, the surface structure of those agglomerates is on a larger scale not homogeneous but very rough.

In the next figure we choose another graphic representation which is more plastic and gives a top view of the investigated surface. To get a better comparison between the two different carbon blacks we choose the same scan area in Figure 10 as in Figure 4. Figure 10a and 10b display a typical agglomerate of N110 particles. In the topographical image of Figure 10a no individual particles can be seen. Figure 10b shows a frictional picture measured simultaneously with topography. In comparison to the topographical image a higher contrast is obtained in the friction mode; grains and grooves are better resolved. The average friction coefficient of carbon black is higher than the one of the mica substrate. This can be recognized by the dif-

ferent grey scale; carbon black particles show up lighter than mica.

This investigations on the surface of carbon black represent only preliminary studies to analyse carbon black-polymer composites. The friction coefficient of carbon black differs by far from that of natural rubber. Therefore, in the friction mode the areas corresponding to natural rubber must show a distinct contrast. In this way, we can extract information about the chemical composition of the sample which is not possible with a conventional AFM.

Figure 11 displays three particles lying close to each other and one single particle. It seems that the three particles are agglomerated because there is only a very small neck between the three bright spots in comparison to the single particle lying beside. The width of the formed agglomerate is about 20 nm corresponding to the average diameter of one particle reported in the literature. Thus the length of the three particle formation should be 60 nm, vs. a measurement of approximately 50 nm. This is also a hint of agglomeration.

The microstructure of N110 is shown in Figure 12. This image looks like Figure 9; the scan area is the same, but the roughness of the microstructure differs by far (see reference height at the left bottom corner of the image). In the left upper corner of this image a new particle begins, separated by a groove from the other one.

To get a better imagination of the microstructure itself and of the difference between the structure of N110 and N762, one scan line of Figure 12 and Figure 9 will be compared in Figure 13. First, the microstructure is rougher for N110 than for N762. Both scan lines show a structure of many edges, corresponding to the layer stacks. As can be seen, the tilt of the layer stacks must be much greater for N110 than for N762 to get a rougher surface. The vertical dimensions are usually in the order of 0.5–1.0 nm (N110) in contrast to 0.2–0.4 nm (N762). The lateral extension of N110 could be estimated to be about 1.0–1.5 nm.

These observations discussed above support a classical model of carbon black. Specific preparation methods made it possible to study carbon blacks intensive by X-ray diffraction and transmission electron microscopy (TEM). On this basis many models have been proposed for the surface structure [20, 21, 22]. A model by Heidenreich [23] illustrating crystallite orientation in carbon black is shown in Figure 14. For the sake of simplicity this is given as a cutaway view

Figure 10a). Topography of a N110 agglomerate recorded in contract force mode with a loading of $1 \cdot 10^{-8}$ N. The grey scale chart covers 45 nm; scan area is $123 \cdot 123 \text{ nm}^2$.

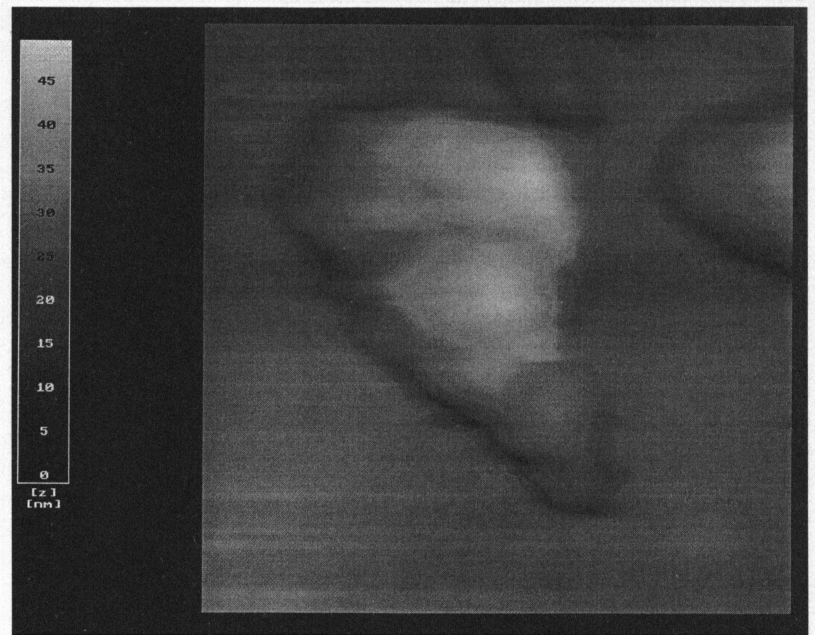


Figure 10b). A frictional force image simultaneously measured with the topographical image and the same loading. The resolution of the agglomerate is better than in topography mode and individual particles can be seen. (The vertical scale is in arbitrary units.)

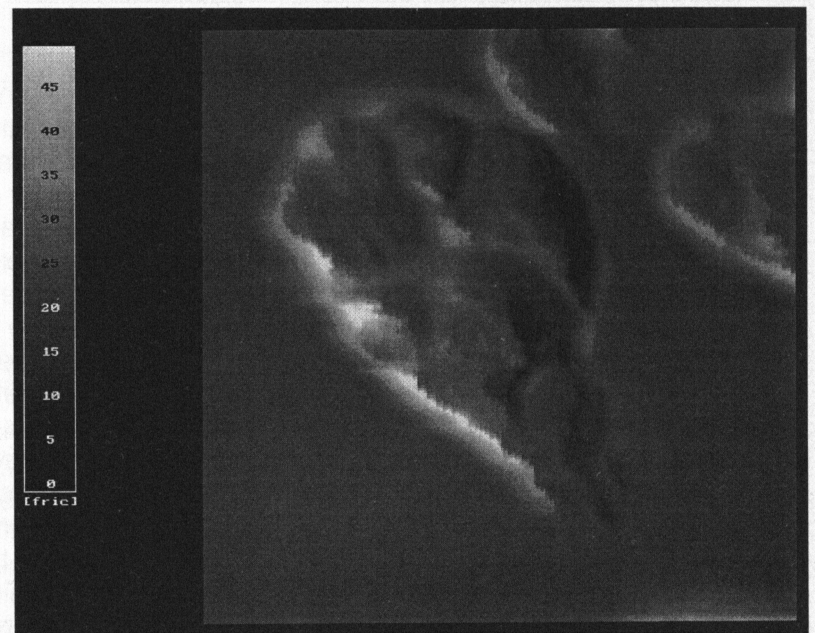
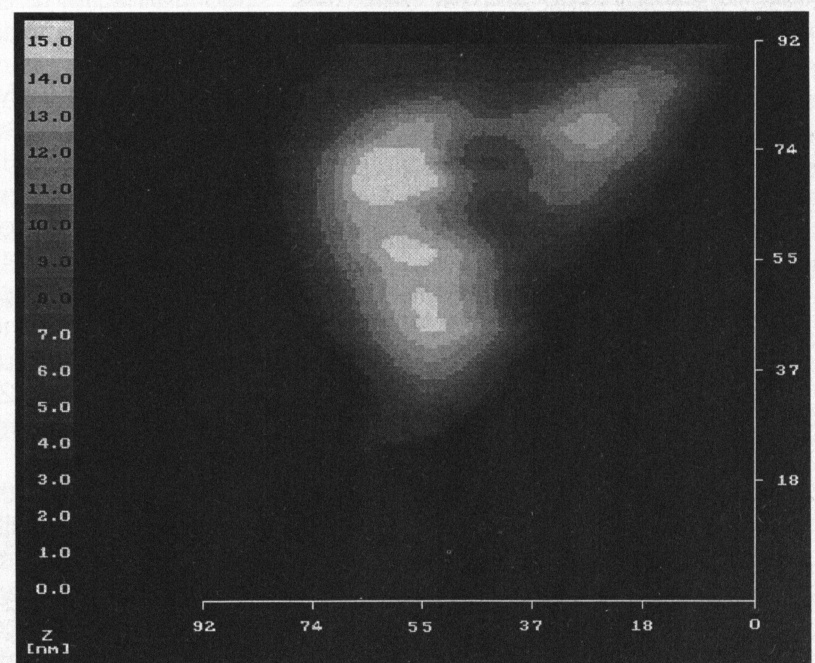


Figure 11. AFM image (top view) of four single carbon black particles (N110) with diameters of 16–20 nm. On the left side there are three agglomerated particles. The grey scale spectrum covers 15 nm; scan area is $92 \cdot 92 \text{ nm}^2$.



of a single spheroidal particle. X-ray diffraction studies have shown that most commercial carbon blacks are made of

crystallites which average about four graphite layer planes. The layer planes are roughly parallel and equidistant. The

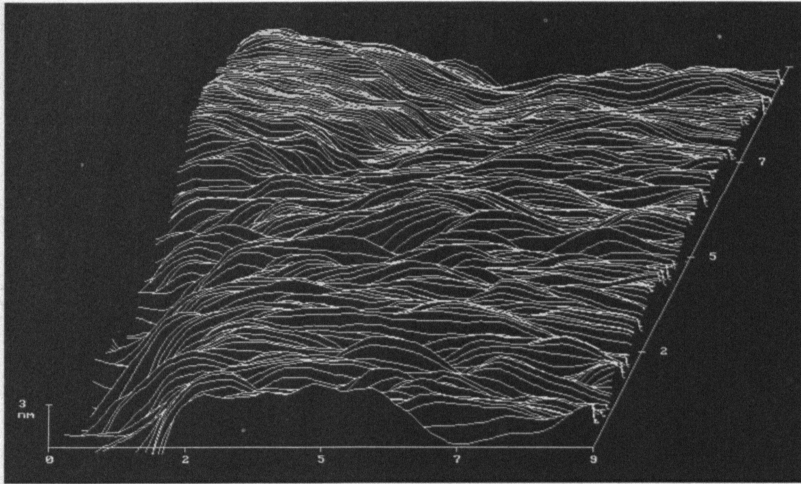


Figure 12. Typical image of the microstructure of N110 carbon black. The image shows crystallites tilted with respect to each other. The surface roughness is smaller than the one of N762 carbon black. The scan area is $9 \cdot 9 \text{ nm}^2$; reference height is 3 nm.

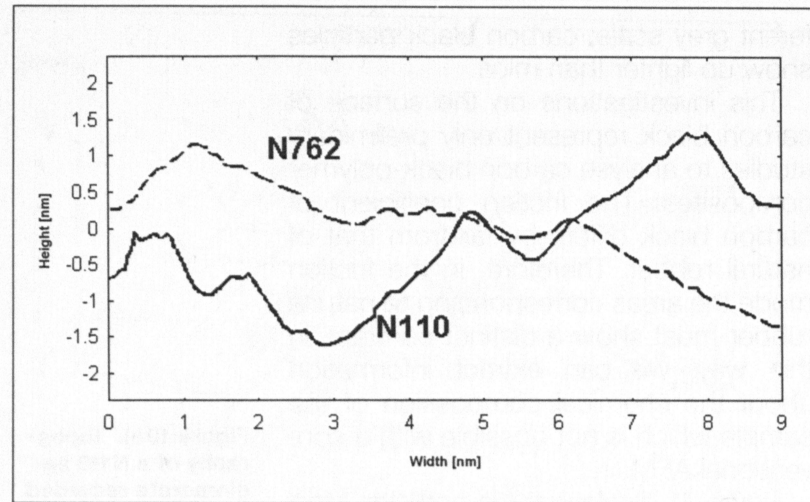


Figure 13. A comparison of scan lines measured at N110 and N762 carbon black. The solid lines represent a scan line of N762 surface shown in Figure 9; the dotted line represents a scan line of N110 surface shown in Figure 12. The lateral dimensions of the crystallites can be estimated to 1.0–1.5 nm for N110 carbon black and to 1.8–2.5 nm for N762 carbon black.

stack height of the crystallites is in the range of 1.1–1.7 nm [18, 23, 24]. The horizontal extension is about 1.5–2.4 nm. The spacing of the layer planes is in the range 0.35–0.37 nm, being larger than in graphite. The thickness of the layer is 0.28 nm.

To connect this model with the reported AFM images, we modeled a surface of tilted square bricks, which should illustrate the graphite layer stacks and form the surface of a carbon black particle (Figure 15). The dashed lines correspond the schematically scan lines made by an AFM on such a surface. The sketch will contribute to a clearer understanding of the interpretation of the AFM images.

As can be seen, the model by Heidenreich is fitting in principle with our measurements, but to understand the different reinforcing behavior of carbon blacks in elastomeres, two additional parameter must be taken into account. The first one

is the lateral size of the graphite layer stack, ranging from 1.0–1.5 nm for N110 and from 1.8–2.5 nm for N762. It is seen in Figure 15 that the tilt is the second important parameter for the correct description of the real microstructure. The two parameters lead to an increase of the specific surface of carbon black with decreasing particle diameter. Thus, more adhesion sites are available for additional crosslink points between natural rubber and carbon black. The edges of the graphite layers may play a further role. They prevent a slipping of the rubber molecules under extensional force to a larger extent than in the case of a flat surface. Altogether, this leads to a better reinforcing effect of the carbon black.

4 Conclusion

In this work an AFM was used for a systematic study of surface topography of carbon blacks. With the AFM the formation of agglomerates can be investigated and the diameter of single particles can be measured. Detailed images of the N762 and N110 carbon black surface corroborate in principle a model of the carbon black corrugation developed by Heidenreich et al. [23], but it is necessary to add some diversifications to this model.

First, it is seen that the lateral dimensions of the graphite layer stacks, building up the carbon structure, change with the investigated type of carbon black. Additional, as a second parameter, the tilt of the graphite platelets with respect to each other must be taken into account.

These two parameters seem to be significant in regard to the reinforcing effect of different carbon blacks. The smaller the individual particle diameter, the less

the lateral extensions and the greater the tilt of the graphite platelets. In fact, both parameters act in the same way, they increase the specific surface of the carbon black. It is well known that the primary particle size of the filler is directly related to its surface area, which is an extensive factor and determines the contact area

Figure 15. Schematic carbon black surface as a result of the interpretation of the AFM images. The graphite crystallites are illustrated by square bricks. The dashed lines above the model are possible scan lines measured by an AFM on such a formed surface.

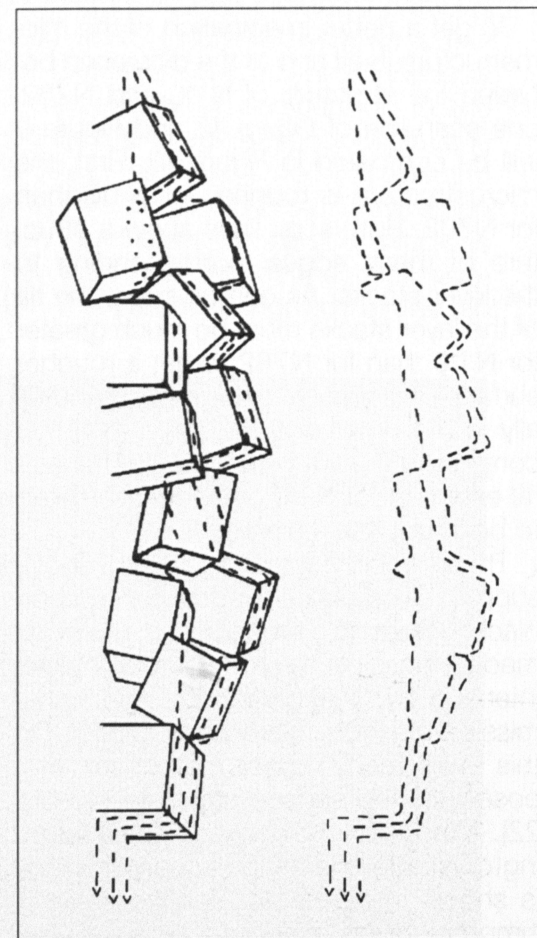
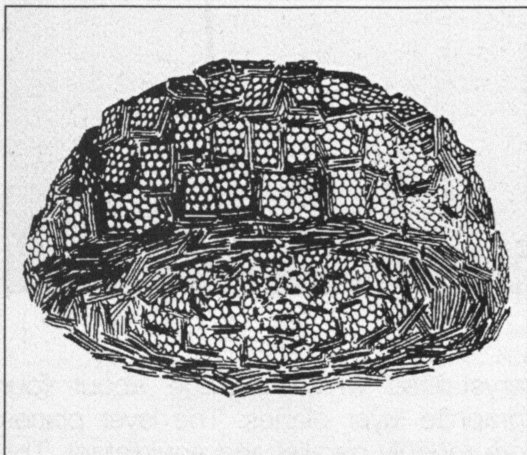


Figure 14. Model of the microstructure of a single carbon black particle [23]. The perspective drawing shows the arrangement of the crystallites. The layer planes are tangential to the particle surface.



between filler and rubber, i.e. it determines the size of the interface between filler and polymer in the composite. Any characteristic of the filled rubber which is related to the interface is strongly affected by particle size or surface area as well as by size and shape of the aggregate.

References

- [1] G. Kraus, *Rubber Chem. Technol.* **38** (1965) 1070.
- [2] G. R. Hamed and S. Hatfield, *Rubber Chem. Technol.* **62** (1989) 143.
- [3] J. B. Donnet and C. M. Lansinger, *Kautsch. Gummi Kunstst.* **45** (1992) 459.
- [4] D. Göritz, W. Niedermeier and J. Stierstorfer, *Proceedings of the Second International Conference on Carbon Black*, Mulhouse, France, (1993) 333.
- [5] G. Binnig, C. F. Quate and Ch. Gerber, *Phys. Rev. Lett.* **56** (1986) 930.
- [6] G. Binnig, H. Rohrer, Ch. Gerber and E. Weibel, *Appl. Phys. Lett.* **40** (1981) 178.
- [7] J. Vancea, G. Reiss, F. Schneider, K. Bauer and H. Hoffmann, *Surf. Sci.* **218** (1989) 108.
- [8] PZT-5A; Staveley Sensors INC, 91 Prestige Park Cir., East Hartford CT 06108.
- [9] W. M. Hess, ACS – Meeting, Rubber Division, New Orleans, USA (1975).
- [10] W. Niedermeier, J. Stierstorfer, S. Kreitmeier, O. Metz and D. Göritz, *Rubber Chem. Technol.* **67** (1994) 148.
- [11] C. M. Mate, G. M. McClelland, R. Erlandsson and S. Chiang, *Phys. Rev. Lett.* **59** (1987) 1942.
- [12] R. Erlandsson, S. Chiang, G. M. McClelland, C. M. Mate and G. Hadziioannou, *J. Chem. Phys.* **89** (1988) 5190.
- [13] O. Marti, J. Colchero and J. Mlynek, *Nanotechnology* **1** (1990) 14.
- [14] F. O. Goodman and N. Garcia, *Phys. Rev. B.* **43** (1991) 4728.
- [15] L.O.T.-Oriol GmbH, Darmstadt.
- [16] Park Scientific Instruments SA, Carouge-Geneve.
- [17] "Was ist Ruß?", Firmenschrift der Degussa AG, Frankfurt (1084).
- [18] J. B. Donnet and C. M. Lansinger, *Kautsch. Gummi Kunstst.* **45** (1992) 459.
- [19] K. Vohwinkel, *Kautsch. Gummi Kunstst.* **39** (1986) 810.
- [20] F. A. Heckman, *Rubber Chem. Technol.* **37** (1964) 1245.
- [21] F. A. Heckman and D. F. Harling, *Rubber Chem. Technol.* **39** (1966) 1.
- [22] D. F. Harling and F. A. Heckman, *Mater. Plast. Elastomeri* **35** (1969) 80.
- [23] R. D. Heidenreich, W. M. Hess and L. L. Ban, *J. Appl. Cryst.* **1** (1968) 1.
- [24] W. G. Peng, M. Strauß, T. Pieper and H. G. Kilian, submitted to *Molec. Phys.*

Authors

Dipl. Phys. W. Niedermeier, H. Raab, Dipl. Phys. J. Stierstorfer, Dr. S. Kreitmeier and Prof. Dr. D. Göritz – Institute of Applied Physics, University of Regensburg.

Hermann-Staudinger-Preis an Burkart Philipp

Professor Dr. Burkart Philipp, der sich um die Förderung der Polymerwissenschaften in herausragender Weise verdient gemacht hat, erhielt den Hermann-Staudinger-Preis 1994 der Gesellschaft Deutscher Chemiker (GDCh). Die Verleihung fand bei der GDCh-Festsitzung am 19. September 1994 anlässlich der 118. Versammlung der Gesellschaft Deutscher Naturforscher und Ärzte in Hamburg statt.

Burkart Philipp ist durch seine wissenschaftlichen Arbeiten auf dem Gebiet der Cellulosechemie, der Polyelektrolyte und der Anwendung von Cellulosederivaten in der Technik international hervorgetreten. Er hat in der ehemaligen DDR eine

Forscherguppe von internationalem Rang aufgebaut und geleitet. Aus dieser Forschergruppe kamen u. a. bedeutende Anstöße zur Entwicklung der modernen Kolloidchemie. In über 700 Publikationen sind die Ergebnisse seiner Arbeiten niedergelegt. Seiner Persönlichkeit und Integrationsfähigkeit ist es zu verdanken, daß die bedeutenden makromolekular ausgerichteten Arbeitsgruppen aus Einrichtungen der Akademie der Wissenschaften der DDR im Zuge der Neugestaltung der Wissenschaftslandschaft in Einrichtungen der Max-Planck-Gesellschaft, der Fraunhofer-Gesellschaft oder der Hochschulen überführt werden konnten. Philipp hat damit wesentlich zur Gestal-

tung der Zukunft der Grundlagenforschung in Deutschland beigetragen.

Philipp wurde 1925 in Pirna geboren. Sein 1947 an der TH Dresden begonnenes Chemiestudium schloß er dort 1952 mit der Promotion bei Kurt Schwabe ab. Vier Jahre später hatte er sich habilitiert und seine Tätigkeit am Institut für Faserstoff-Forschung (später Polymerenchemie genannt) der Akademie der Wissenschaften zu Berlin begonnen. Er stieg bis zum Direktor dieses Institutes auf. Seine wissenschaftlichen Arbeiten wurden durch Auszeichnungen der Chemischen Gesellschaft der DDR gewürdigt.

Prof. Dr. sc. nat. Kurt Thinius verstorben

Erst jetzt wurde der Redaktion bekannt, daß Prof. Dr. Kurt Thinius am 6. Juli 1994 im Alter von 91 Jahren verstorben ist.

Seine großen Verdienste als Polymerforscher lassen sich anhand zahlreicher Veröffentlichungen und ca. 100 Patentanmeldungen nachweisen.

Die von ihm schon in den Zwanziger

Jahren begonnenen Arbeiten stellten die Ergebnisse auf den Gebieten Weichmacher und ihre Wirkung, Alterung und Stabilisierung von Polymeren, Verträglichkeit, Klebstoffe und Klebtechnik dar.

Nicht zu vergessen ist das Bemühen von Prof. Dr. Thinius um die Normung und Standardisierung der Polymere.

Er hielt in Leipzig Vorlesungen über „Makromolekulare Chemie“ und veröffentlichte in der von ihm mitgegründeten Zeitschrift „Plaste und Kautschuk“ 200 Originalarbeiten unter seinem Namen oder gemeinsam mit seinen Mitarbeitern.